

The Shear-force/Ultrasonic Near-field Microscope: A Nanometrology Tool for Surface Science and Technology

A. La Rosa, N. Li, and K. Asante

Physics Department, Portland State University, Portland, OR 97207, USA.

ABSTRACT

This paper describes recent results obtained with the Ultrasonic/Shear-Force Microscope (SUNM), an analytical tool suitable for investigating the quite different dynamic displayed by fluid-like films when subjected to mesoscopic confinement and while in intimate contact with two sliding solid boundaries. The SUNM uses two sensory modules to concurrently but independently monitor the effects that fluid-mediated interactions exert on two sliding bodies: the microscope's sharp probe (attached to a piezoelectric sensor) and the analyzed sample (attached to an ultrasonic transducer). This dual capability allows correlating the fluid-like film's viscoelastic properties with changes in the probe's resonance frequency and the generation of sound. A detailed monitoring of sliding friction by ultrasonic means and with nanometer resolution is unprecedented, which opens potential uses of the versatile microscope as a surface and subsurface material characterization tool. As a *surface* metrology tool, the SUNM presents a potential impact in diverse areas ranging from fundamental studies of nanotribology, confinement-driven solid to liquid phase transformation of polymer films, characterization of industrial lubricants, and the study of elastic properties of bio-membranes. As a *sub-surface* metrology tool, the SUNM can be used in the investigation of the elastic properties of low- and high-k dielectric materials, piezoelectric and ferroelectric films, as well as quality control in the construction of micro- and nano-fluidics devices.

Keywords: Ultrasonic, shear-force, nanometrology, near-field, confined fluids, acoustic, sub-surface characterization, nanochannels.

1. INTRODUCTION

Surface phenomena involving mesoscopic fluid-like films constrained between solid surface boundaries present an exquisite source of experimental measurement challenges and constitute at the same time one of the problems in condensed matter not yet well understood at the fundamental level. The experimental difficulty resides in that (i) the films are buried between two sliding bulk phases, and (ii) there is relatively little material available for analysis. Such confinement occurs because the profile of a common solid surface is very irregular at mesoscopic scales, thus resembling one composed of many asperities of different sizes (see schematic in Fig. 1a). Since the physical properties of confined fluids differ greatly from their bulk ones,^{1,2} it is believed that they can play an important role

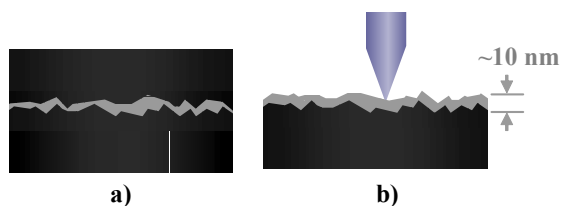


Fig.1 a) Two surfaces in contact leave fluid-like films confined to mesoscopic regions, whose enhanced rheological properties are expected to play a major role in friction phenomena. **b)** A sharp probe, acting as a nanometer-sized asperity, allows the study of fundamental micromechanical and tribological properties of surfaces and interfaces with nanometer lateral resolution.

in sliding friction.^{3,4} The many intervening interactions in such solid-liquid-solid systems (van der Waals, capillary, electrical, and viscous forces, to name just a few) make their study challenging.

To simplify the problem, one approach opts for reducing the area of one of the surfaces in contact, thus resembling the interaction of one surface with another that has just one or a few asperities, as schematically shown in Fig. 1b. (Other significant approaches are: the surface-probe apparatus^{5,6} that measures both static⁷ and dynamic^{1,8} forces between atomically flat surfaces; the quartz microbalance technique;⁹ and computer simulations.¹⁰) The importance of investigating single asperity contacts in studies of the fundamental micromechanical and

tribological properties of surface and interfaces has long been recognized.^{2,11,12} The resulting scenario in this approach resembles very much the experimental arrangement encountered in scanning probe microscopes as seen, for example, in atomic force microscopy (AFM)^{13,14} and near-field scanning optical microscopy (NSOM).^{15,16} As a matter of fact, AFM was the first technique to be used to study friction at the nanometer scale. In this technique, a sharp stylus is laterally dragged along the surface while monitoring its lateral bending caused by the frictional force acting between the sharp probe and the specimen. The smaller the bending experienced by the probe, the lower the frictional force.^{17,18}

A limitation of the AFM technique is that it senses the effects that frictional forces cause *only* on the AFM probe, but information provided by effects on the sample is lost. How is the energy transferred to the sample before being converted to heat? Is such transfer caused by electrical interactions or by phonons? What is the role of (as well as the effects on) the adsorbed fluid-layer? Such issues are generally difficult to address experimentally, not only because of the delicate nature of the phenomena, but also because it is difficult to implement experiments that admit unambiguous interpretation. Capturing simultaneously as much information resulting from the interaction region as possible would be optimal.

The recently introduced Shear-force/Ultrasonic Near-field Microscope (SUNM)¹⁹ addresses properly these demands. It uses a piezoelectric tuning fork sensor (attached to a sharp stylus) and an ultrasonic transducer (attached to the sample under analysis), which allows a direct, simultaneous, and concurrent monitoring of the effect of the fluid-mediated surface interactions on the probe, the fluid itself, and on the sample. In addition to its *surface* metrology capabilities, the SUNM also has potentials as a *sub-surface* material characterization tool. Indeed, since the ultrasonic wave (generated locally just above the surface by the microscope's sharp tip) travels through the analyzed sample (towards the acoustic transducer placed underneath), materials with different physical properties (for having subsurface defects, for example) will present dissimilar acoustic coupling efficiencies.

Current efforts in our laboratory point towards obtaining a full understanding of how sound propagates within the SUNM experimental setup (is it ballistic, or, do stationary standing waves establish inside the sample?), exploiting its capability for distinguishing viscous from conservative interactions, and exploring its ability for nanometer lateral resolution imaging of sub-surface elastic properties.

2. THE SHEAR-FORCE/ULTRASONIC NEAR-FIELD MICROSCOPE

A detailed description of the SUNM has been reported elsewhere.¹⁹ Very succinctly, Fig.2 displays three

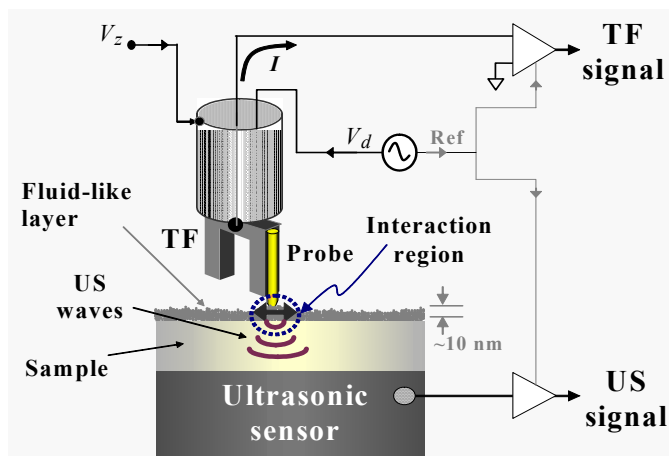


Fig. 2 The *Ultrasonic/Shear-force Near-field Microscope (SUNM)*. The tip of a sharp probe laterally oscillates while interacting with a (polymer or water) layer adsorbed to the sample's surface. On stimulation, the viscoelastic properties of the layer engender ultrasonic waves, which are detected with an ultrasonic transducer located underneath the sample. The ability to correlate the effects that frictional forces exert on the probe and on the adsorbed layer (both measured independently) constitutes one of the attractive features of the SUNM.

distinct sections of the experimental arrangement: the probe and the specimen (at the center), the tuning fork-based detection for monitoring the probe's mechanical response (displayed in the upper side), and an ultrasonic transducer, in intimate contact with the sample, to detect the waves engendered by the laterally oscillating probe (displayed in the lower side). In the experiments reported here the probe is an uncoated, chemically etched, tapered optical fiber, held attached to one of the tines of a commercially available quartz tuning fork (TF). Alternatively, functionalized probes (chemically coated probes, or near-field optical microscope probes, for example) could be used instead to gain further characterization capabilities.

A signal generator drives the TF with an ac voltage of amplitude V_d , (typically set to $10 \text{ mV}_{\text{rms}}$), which causes the tines and the probe to oscillate laterally. The corresponding generated current I (this is due to the piezoelectric properties of the TF) is synchronously detected with a lock-in amplifier whose output will be referred to

here as the “TF signal;” this signal gives an indication of the probe’s mechanical oscillation amplitude. A frequency sweep helps determine the resonance frequency of the combined TF/probe system, which is used during the probe’s approaching and retraction from the sample’s surface. A V_z voltage applied to a piezo tube, to which the TF is attached, controls the vertical position of the probe with sub-nanometer resolution.

While driving the TF at its resonance frequency, the probe is brought gradually closer to the sample’s surface. No major variation in the TF signal is observed until the tip encounters the boundary of the layer typically found adsorbed to the sample’s surface at ambient conditions, which causes the TF signal to suddenly decrease; simultaneously, the oscillatory motion of the now immersed probe engenders acoustic waves that subsequently propagate downwards through the sample and towards the ultrasonic transducer. The ultrasonic transducer’s signal is amplified and synchronously detected with an independent lock-in amplifier referenced to the TF’s driving frequency; the output of this lock-in is referred to here as the “ultrasonic-signal”. Even though this experiment was initially conceived to detect the sound produced by the intermittent solid-solid contact between the probe and the sample’s surface (which is expected to happen after bringing the tip close enough to the sample’s surface) the ultrasonic sensor demonstrated sufficient sensitivity to detect sound waves even when the tip was being retracted from the surface. It is also worthwhile to highlight that this detection was possible without using exceedingly high oscillation amplitudes; for example a signal to noise ratio of 10 is obtained with 5 nm amplitude of oscillation at the time when the probe gets immersed into the adsorbed layer, and (depending on the surface conditions) increases greatly as the tip approaches the sample.

3. CHARACTERIZATION OF MESOSCOPIC FLUID-LIKE FILMS

3.1 Correlation between the viscoelastic properties of mesoscopic films and phonon generation

Figure 3 displays a time evolution of the TF and ultrasonic signals as the probe makes excursions in and out from the sample’s adsorbed layer while oscillating at its resonance frequency and with amplitude of ~ 5 nm. The high correlation between these two signals is evident throughout the four intervals shown in this graph. During the interval marked with the numeral 1, while the probe advances toward the surface (the V_z voltage driving the approach is not shown) the maximum TF and minimum ultrasonic signal levels remain unchanged. When the probe encounters the layer boundary, as evidenced by the sudden decrease in the TF signal, the ultrasonic signal

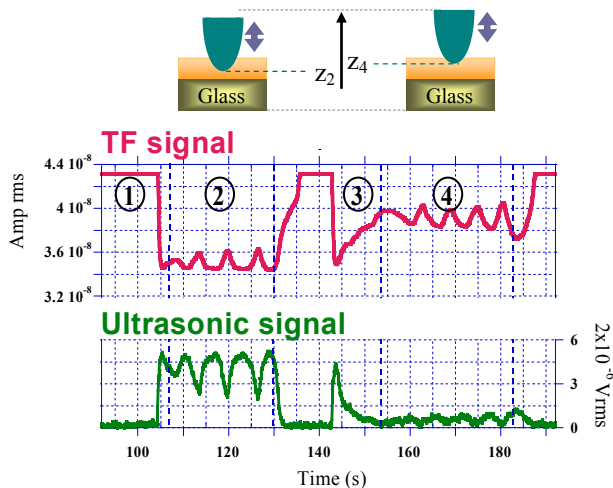


Fig. 3 Time evolution of the TF and ultrasonic signals as the tip is forced to make vertical excursion inside the sample’s adsorbed layer.

accordingly increases. During interval #2, the tip remains immersed in the layer but forced to make short vertical excursions, in and out, around a position z_2 near the surface; changes in the TF signal are accompanied by quite clear variations of the ultrasonic signal. Notice, the closer the tip is to the surface, the smaller the TF signal, and the greater the intensity of the sound.

The observed increasing intensity of sound at closer distances from the surface can be ascribed to a distance dependence of the layer’s viscoelastic properties. Such an interpretation, however, requires a viscoelastic coefficient for a water film much greater than the bulk values,¹⁹ which is conceivable to happen in confined mesoscopic fluids.^{1,2} This may be the reason why the SUNM surpassed its initial expectations for detecting the sound produced by intermittent hard contact between the solid tip and the solid sample; it turns out that sound is detected even when such solid-solid contact does not take place. The very high

viscoelasticity of the layer acts, then, as an amplifier of the waves generated by the laterally oscillating probe immersed in the fluid layer, thus allowing them to be detected as well. This is confirmed during interval #3 where, even when the tip is being retrieved from the surface (so no hard contact between the probe and the sample exists), still a clear ultrasonic signal is detected. (The deformable meniscus formed around the probe can also have a significant influence on the probe’s lateral motion; to diminish this effect, our group is currently performing experiments with the tip immersed in liquids) Finally, during interval #4 the tip makes incursions similar to those

performed during interval #2, but this time at a distance z_4 further away from the surface. For similar amplitude changes in the TF signal, the variations in the ultrasound signal are much lower.

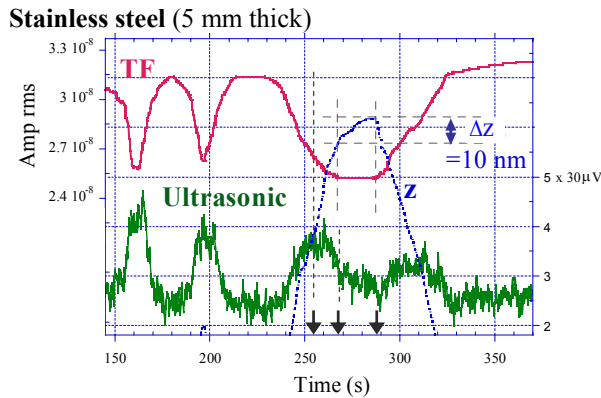


Fig. 4 Time evolution of the TF (magnitude) and ultrasonic (magnitude) signals as the probe is forced to make vertical excursion in the sample's adsorbed layer. "Positive" correlation (in the $t < 255$ s interval) as well as "negative" correlation (just after $t = 255$) are observed. The relative vertical position of the probe, z , as a function of time (dashed line) is also shown ($240 < t < 320$ s interval).

closer to the surface the TF signal decreases, but the ultrasonic signal first remains constant and then decreases. At this stage ($t = 265$) the TF signal has reached its minimum value, apparently because the tip is touching the surface. The probe may still have some lateral motion, since an ultrasonic signal above the ground level is still detected. Subsequently, from $t = 265$ to 285, (the time interval marked by the arrows), an attempt was made to vertically advance the tip an extra 10 nanometer (as a consequence the tip exerted a pressure on the surface) with the result of an unchanged TF signal and (if not constant) a slight decrease in the ultrasonic signal. That is to say, a solid-solid contact between the probe and the surface did not produce an increase in sound intensity; on the contrary, the ultrasound signal slightly decreases. This latter aspect is the source of current tribology studies in our laboratory. Aiming to verify whether this result is a consequence of the sample's roughness, tests using atomically flat samples produce similar affects. This latter aspect is the source of current tribology studies in our laboratory. It appears, then, that the increasing or decreasing of the ultrasonic signal as the probe makes contact with the surface is a characteristic associated with the particular state of the local sample's properties.

In short, the SUNM identifies in the probe-sample interactions (mediated by the mesoscopic adsorbed layer) two distinct regions. In the region far from the surface (but while the tip remains immersed in the adsorbed layer), a "negative" correlation between the TF and the ultrasonic signal does exist, regardless of the type of sample analyzed. A decrease in the TF signal (i.e. a decrease in the probe's amplitude of vibration) is accompanied by an increase in the intensity of the ultrasound. The loss of mechanical energy by the probe appears as an elastic vibration (sound) at the fluid layer and propagates, through the sample, towards the ultrasonic transducer. Precise monitoring of this interaction should provide the basis for an accurate modeling of the viscoelastic properties of the mesoscopic adsorbed layer. On the other hand, in the near-region (the last 10 nanometer), the experiments reveal that the (positive or negative) correlation between the TF signal and the ultrasonic signal depends on the local properties of the material. Occasionally, the hard contact between the probe and the sample produces higher intensities of sound (as well as a higher TF signal, as will be seen in the results of Fig. 5 below), which suggests that, in such a case, an intermittent contact (producing non-linear effects in the probe's oscillations) is the probable cause of these effects. On other occasions, the close proximity between the probe and the sample rather causes the probe to come to rest (or to a minimum level of oscillation), causing the ultrasonic signal to decrease as the probe approaches the sample. It is revealing to verify that a further push of the probe into the sample did not cause a more intense ultrasonic signal, rather a slight decreasing (the less lateral motion, the lower ultrasonic signal). In this regard, the SUNM offers a great opportunity to investigate the role of phonons as a dissipation channel in friction phenomena at the nanometer level.

We have found that, as far as the probe is not too close to the sample, the "negative" correlation between the TF and ultrasonic signals (that is, one decreasing while the other increasing, and vice versa), is a common behavior observed when analyzing different types of samples: glass, atomically flat mica, silicon wafers and stainless steel, with thickness values ranging from less than a millimeter up to 5 millimeter. However, depending on the local properties of the sample (we do not yet know the exact reason), the correlation switches signs. This can be seen in Fig. 4, which corresponds to a 5 millimeter-thick stainless steel sample.

The graph displays the time evolution of the TF and ultrasonic signal while the tip is immersed in the adsorbed layer and forced to make vertical excursion (similar to what was described for Fig.3). In interval from $t = 150$ s to $t = 255$ s, the "negative" correlation between the signals is observed. But, between $t = 255$ s and $t = 265$ s, as the tip is brought closer to the surface the TF signal decreases, but the ultrasonic signal first remains constant and then tends to decrease. But, between $t = 255$ s and $t = 265$ s, as the tip is brought

3.2 Spectral characterization of probe-fluid layer interactions

Another compelling result revealed by the SUNM is the correlation between the increase in the ultrasonic signal and the shift in the resonance frequency experienced by the probe. This result is summarized in figures 5 and 6.

Figure 5 shows spectra taken at different probe-sample distances, starting with the tip positioned far away from the sample (curve F with open squares), then while approaching the sample (curve G with open circles, and H with open triangles), and finally during a more gradual retraction (curves *m* to *v*, in alphabetic order). In these results, the TF signal is the magnitude of the rms value of the ac current supplied by the TF, while the ultrasonic signal is the output of the ultrasonic transducer fed to a one-phase lock-in amplifier; this explain the disagreement in the peak position between the corresponding TF and ultrasonic spectra. During the approaching process it is difficult to acquire stable spectra just after the probe encounters the adsorbed layer (the acquisition time for each spectrum was 50 seconds). Here, spectrum G corresponds to a tip already well immersed into the contamination layer, and probably already in contact with the solid sample's surface. In effect, an attempt for making a deeper incursion of the probe into the sample (curve H, open triangles) causes a further increase of the TF signal rather than a decrease (as it would have happened if the tip were immersed only in the contamination layer). We expect, therefore, that the probe is in solid-solid contact with the surface. A peculiar behavior occurs at this stage (after acquiring curve H). When the probe is pushed further into the sample, the peak amplitude of the TF signal does not change any more; rather a series of frequency response curves (corresponding to slightly different V_z voltage, and indicated with

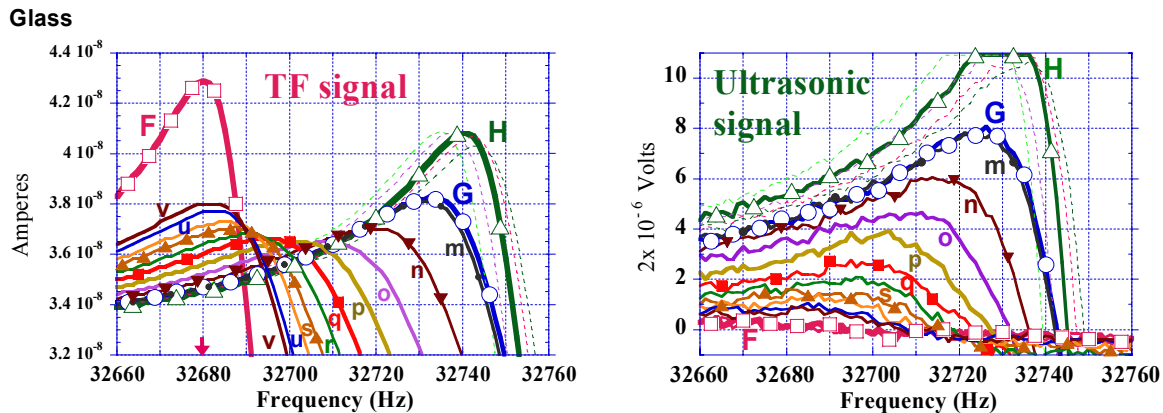


Fig. 5 Frequency response of the signals at different probe-sample distances. Spectrum F recorded when the probe was outside the adsorbed layer (the arrow indicates the frequency at which the spectrum F has its peak); G and H taken during the approach; spectra labeled in alphabetic order from “m” to “v” were taken while retracting the probe.

dashed lines in the figure) gather around spectrum H; these spectra do not display appreciable resonance frequency shift either. It appears, then, that the tip clamped into the sample and the resonance frequency is not anymore affected appreciably by the extra tension force at the tip. The latter however significantly affects the intensity of the ultrasonic signal, as can be noticed in the figure that some spectra get out of the measurement scale.

When the probe is retracted from the surface, the spectra at different probe-sample distance are very stable. For example, spectrum *m* reproduces very well the spectrum G (the one taken during the approach) in both instances, in the registered TF signal and in the ultrasonic counterpart. This illustrates the existent close correlation between the two independently acquired signals and their reproducibility; at a given probe-sample distance they provide the same signal levels. As the probe further retracts (curves “m” to “v”) a monotonic decrease in the probe’s resonance frequency is accompanied by a monotonic decrease in the sound peak intensity which continues until the probe is completely out of the adsorbed layer (curves F).

The different behavior of the TF signal before and after the spectrum “q” (filled squares curve) suggests defining this stage as the $z=0$ reference; the point where the tip stops making solid-solid contact with the surface during the retraction. After making this assumption, it was instructive to verify whether the tip-adsorbed layer interaction keeps causing a shift on the probe’s resonance frequency. That this is indeed the case is shown in Fig. 6 (the data is the same displayed in Fig. 5), where a frequency shift of 15 Hz is observed between spectra q and spectra v (after retracting the probe by 80 nm). Notice also that the intensity of the ultrasonic signal varies

accordingly with the frequency shift; the greater the resonance frequency shift, the greater the intensity of the sound. This observation is very compelling since gives clues on the constitutive nature of the adsorbed film. It not only

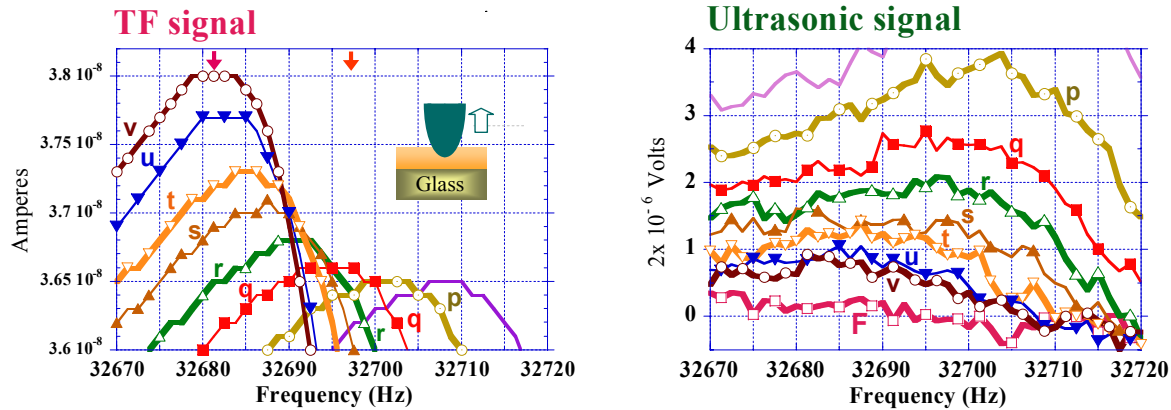


Fig. 6 Correlation between resonance frequency shifts and increases in the sound intensity. These two graphs are a zoom-in of the graph displayed in Fig.5 (labels keep the same meaning), emphasizing the resonance frequency shift of the probe caused by its interaction with the sample's adsorbed layer (left), which correlates with the increase in the ultrasonic signal (right). The arrows indicate the frequencies at which the spectra "F" (not shown) and "q" have their peak values. A frequency shift of ~15 Hz (spectra q and v) is obtained when the tip retracted 80 nm.

produces a damping force, it is also the source of an elastic restoring force.

4. OTHER POTENTIAL APPLICATIONS OF THE SUNM

Many interesting applications can be envisioned exploiting the scanning imaging capabilities of the SUNM. The semiconductor industry, for example, is heavily investing in the search for new materials that can keep pace with the continuous trend of electronic device miniaturization. **Low-k dielectrics** (to reduce the interconnection RC delay) as well as **high-k dielectrics** (relevant to the next generation of high-k CMOS gates) are materials under intense investigation and their elastic and electrical properties will need to be characterized at high lateral resolution. This is precisely the terrain of the versatile SUNM. Indeed, a sharp metallic probe in the SUNM can serve as an electrical electrode which can fulfill the requirements for both elastic and electrical characterization simultaneously.

In addition, the more gentle characterization involved in the SUNM (it does not require indentation of the sample, as necessary in other ultrasonic techniques) can make the new technique SUNM much more attractive.

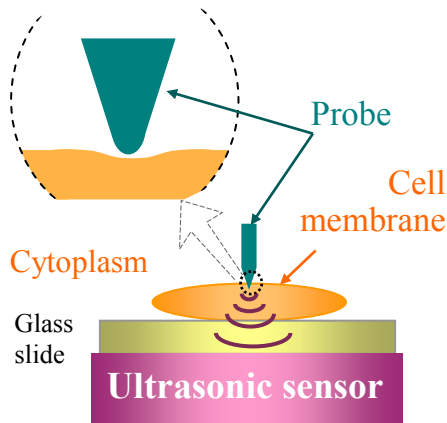


Fig. 7 Schematic view of a sharp probe approaching a cell membrane to locally perturb and characterize its elastic properties (Adapted from Ref 22). The SUNM can exploit its additional ultrasonic sensing capability to monitor the membrane's dynamic mechanical responses by placing the ultrasonic transducer underneath the glass slide.

Ferroelectrics are attractive materials used in combination with integrated circuit technology. New devices such as memory elements, microantennae, or phase shifters for telecommunication and microwave technology, as well as MEMS, use ferroelectric materials in thin film, thick film, or bulk forms respectively. But there still much to do to understand the formation of the devices' ferroelectric domains at the submicron and nanometer scales.²⁰ Ultrasound techniques, in general, offer an additional sample characterization parameter (identification of ferroelectric domains in this case) impossible to obtain with other scanning probe techniques.

Biomembranes have specific and well-regulated mechanical properties, which are not yet well understood (mainly due to the high complexity of living systems). Their structure and mechanical properties can be studied by fluorescence microscopy²¹ and AFM (Fig. 7)²² methods. Theoretical models link the elasticity of domains to the shape adopted by membranes and the formation of particular domain patterns.²³ The former has lateral resolution limitations imposed by diffraction

effects, while for the latter, although it offers greater lateral resolution, image interpretation and associated theoretical models are still in their infancy: the information obtained from only the sharp probe may not be sufficient to characterize the properties of membranes fully. The SUNM, however, has an additional ultrasonic detection capability to directly monitor the probe-membrane interaction effects on the membrane itself, which can provide useful complementary information in the studies of the membrane's mechanical properties. In addition, when a near-field optical probe is used in the SUNM setup, an additional optical characterization with optical sub-wavelength lateral resolution will be possible.

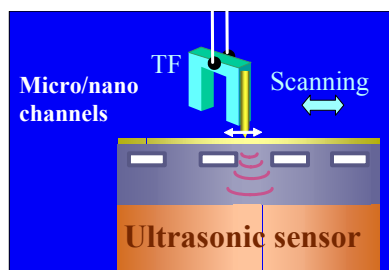


Fig.8 Proposed arrangement to monitor the presence and quality of nanochannels using the SUNM.

applications in fields that require controlling the flow of small volumes of fluid, including (electrophoresis) DNA separation. The embedded nature of nanochannels makes difficult to evaluate their quality and reproducibility. A straightforward arrangement using the SUNM would allow monitoring the quality of nanofluidic devices, based on the contrast in the detected ultrasound signal caused by the hollow structure; a truly subsurface characterization application (Fig. 8).

5. REFERENCES

- ¹ S. Granick, *Science* **253**, 1374-1379 (1991).
- ² Michael Urbakh, Joseph Klafter, Delphine Gourdon & Jacob Israelachvili, *Nature* **430**, 525-528 (2004).
- ³ B. Bhushan, J. N. Israelachvili and U. Landman, *Nature* **374**, 607-616 (1995).
- ⁴ Gang He, Martin H. Müser, Mark O. Robbins, *Science* **284**, pp. 1650-1652 (1999).
- ⁵ D. Tabor and R. Winterton, *Proc. R. Soc A* **312**, 435-450 (1969).
- ⁶ J. Israelachvili, P. M. McGuigan and A. M. Homola, *Science* **240**, 189 (1988).
- ⁷ J. Israelachvili, *Chemtracts-Analyt. Phys Chem.* **1**, 1-12 (1989).
- ⁸ J. Klein, D. Perahia and S. Warbug, *Nature* **352**, 143-145 (1991).
- ⁹ J. Krim, D. H. Solina, R. Chiarello, *Phys. Rev. Lett.* **66**, 181-184 (1991).
- ¹⁰ U. Landman, R. N. Barnett, H. -P. Cheng, C. L. Cleveland, and W. D. Luedtke, in *Computations for the Nano-Scale 75-113* (eds Bloohl, P. E. Joachim and A. J. Fisher). Kluwer Dordrecht, 1993.
- ¹¹ N. Gane and F. P. Bowden, *J. Appl. Phys.* **39**, 1432-1435 (1968).
- ¹² M. D. Pashley, J. B. Pethica and D. Tabor, *Wear* **100**, 7-31 (1984).
- ¹³ Atomic Force Microscopy senses the topography of a sample surface with a sharp pyramid attached to a cantilever. Sharp tips are able to provided atomic topographic lateral resolution.
- ¹⁴ Dror Sarid, "Scanning Force Microscopy: With Applications to Electric, Magnetic and Atomic Forces," Oxford University Press (1994).
- ¹⁵ The Near-field Scanning Optical Microscopy (NSOM) uses a sharp metal-coated tapered optical fiber to sense the topographic and optical properties of surfaces. The probe is coated with metal except at its very apex where a sub-wavelength aperture is left open to deliver light to the sample very locally. The sub-wavelength aperture allows obtaining better lateral resolution than conventional optical microscopy (whose ultimate resolution is of the order of the wavelength of light used in the analysis). NSOM's ability to correlate topographic and optical information, obtained simultaneously, is one of its main advantages.
- ¹⁶ M. A. Paesler and P. J. Moyer, "Near-Field Optics: Theory, Instrumentation and Applications," John Wiley and Sons, Inc., New York (1996).
- ¹⁷ G. M. McClelland and J. N. Glosli, in "Fundamentals of Friction: Microscopic and macroscopic processes" Edited by I. L. Singer and H. M. Pollack, p. 405, Kluwer, Dordrecht (1992).
- ¹⁸ C. M. Mate, "Force microscopy studies of the molecular origins of friction and lubrication," *IBM J. Res. Develop.* **39**, 617-627 (1995).
- ¹⁹ A. H. La Rosa, R. Nordstrom, X. Cui, J. McCollum, and Nan Li; "The Ultrasonic/Shear-Force Microscope: Integrating Ultrasonic Sensing into NSOM," *Rev. Sci. Instrum.* **76**, 093707 (2005).

-
- ²⁰ X. X. Liu, R. Heiderhoff, H. P. Abicht and L. J. Balk, "Scanning near-field acoustic study of ferroelectric BaTiO₃ ceramics," *J. Phys. D: Appl. Phys.* **35**, pp. 74-87 (2002).
- ²¹ T. Baumgart, S. T. Hess and W. W. Webb, "Imaging coexisting fluid domains in biomembrane models coupling curvature and line tension," *Nature* **425**, pp. 821-4 (2003).
- ²² Tai-Hsi Fan and Andrei G. Fedorov, "Analysis of Hydrodynamic Interactions during AFM Imaging of Biological Membranes," *Langmuir* **19**, pp. 1347-1356 (2003).
- ²³ M. Seul and D. Adelman, "Domain shapes and patterns, "The phenomenology of modulated phases," *Science* **267**, pp. 476-483 (1995).
- ²⁴ M. J. Lercel and H. G. Craighead, A. N. Parikh, K. Seshadri, and D. L. Allara, "Sub-10 nm lithography with self-assembled monolayers," *Appl. Phys. Lett.* **68**, pp. 1504-6 (1996).